In Vitro and In Vivo Targeting of Radiolabeled Monovalent and Divalent Haptens with Dual Specificity Monoclonal Antibody Conjugates: Enhanced Divalent Hapten Affinity for Cell-Bound Antibody Conjugate

Jean-Marc Le Doussal, Marie Martin, Emmanuel Gautherot, Michel Delaage, and Jacques Barbet

Immunotech S.A., Campus de Luminy, Marseilles, France

A method of pretargeted immunolocalization of a mouse cell subset, using dual specificity monoclonal antibody conjugates and labeled divalent haptens, is described. Conjugates were prepared by coupling $F(ab')_2$ fragments of an antibody specific for the allelic mouse B cell antigen Lyb8.2, to Fab' fragments of an anti-2,4-dinitrophenyl antibody. Divalent and monovalent haptens were obtained by coupling dinitrophenyl to peptides or to diethylene-triamine-pentaacetic acid. In vitro, divalent haptens bind with higher affinity to mouse spleen lymphocyte-bound than to excess soluble conjugate (affinity enhancement). In vivo, localization of ^{125}I- or ^{111}In-labeled divalent haptens in mouse spleen is much higher than that of the monovalent analogs. Thus, using divalent haptens, a new kind of specificity to target cells was achieved, suggesting that affinity enhancement may improve target to background ratios in radioimmunoscintigraphy.

J Nucl Med 30: 1358–1366, 1989

Recently, the use of low molecular weight tracers, such as indium chelates, associated with dual specificity antibody conjugates (DSC), combining antibodies (or fragments) to the target cells with high affinity antibodies (or fragments) to the indium chelate (dissociation constant in the n*M* range), has been proposed for in vivo radioimmunolocalization and radioimmunotherapy (*1*). Increased uptake ratios and faster localization of the tracer are expected, since the radioactivity would be associated to low molecular weight structures capable of fast distribution through body tissues and rapid clearance (*2*). Images may then be recorded sooner after injection with more radioactive counts than with previous techniques, especially when using short half-life isotopes. Similarly, fast localization and rapid clearance of excess radioactive isotopes would reduce damage to normal cells and tissues in radioimmunotherapy.

The critical parameter of such procedures is the affinity of the DSC towards the hapten. Indeed, when the affinity is too strong, the tracer is effectively trapped by excess circulating DSC: its specific localization and its clearance are impaired (*3*). If this affinity is too low, no specific localization would be obtained. To take advantage of the theoretical potential of the method, excess DSC should be removed from the circulation prior to injection of the tracer (*4*).

Another solution would be to use tracers with higher affinity to cell-bound than to unbound DSC. We propose that this kind of selectivity may be achieved by using divalent or multivalent haptens. Indeed, some natural multivalent ligands bind more tightly to multivalent receptors than the corresponding monovalent ligands [e.g., binding of agregated IgG to the polymeric Fc receptor (*5*), or Clq binding to immune complexes (*6*)]. Similarly, synthetic multivalent ligands for receptors such as the DNA (*7*), or opioid receptors (*8*) have been described as binding their receptors with increased affinity as compared to the monovalent ligand. In this paper, using a mouse B cell antigen as a model system, iodine-125- (^{125}I) or indium-111- (^{111}In) labeled divalent

Received Sept. 1, 1988; revision accepted Mar. 30, 1989.

For reprints contact: Jacques Barbet, Immunotech S.A., Luminy Case 915, 13288 Marseille Cedex 9, France.

haptens were derivatized from dinitrophenyl (DNP) and targeted to BALB/c mouse spleen lymphocytes in vitro and in vivo using a monoclonal antibody conjugate with specificity to the mouse Lyb8.2 antigen and DNP.

MATERIALS AND METHODS

Animals

Male BALB/c (Lyb8.2$^+$) and DBA/2 (Lyb8.2$^-$) mice, 6–8 weeks old, were obtained from IFFA CREDO (Lyon, France). The mouse strain distribution of Lyb8.2 antigen has been described previously (*9*).

Monoclonal Antibodies and Fragments

Clone CY34, secreting the anti-Lyb8.2 monoclonal antibody (*9*), a mouse IgG_1, was obtained through the Cell Distribution Center at the American Type Culture Collection (ATCC, Rockville, MD); clone U7.27, secreting the anti-DNP monoclonal antibody, a mouse IgG_{2a}, was kindly provided by Dr. Z. Eshhar, (Weizmann Institute, Rehovot, Israel); clone G7A5, secreting the anti-melanoma monoclonal antibody, a mouse IgG_1, was obtained from Dr. J.F. Doré, (INSERM, Lyon, France), and clone 679MC7, secreting the anti-histamine monoclonal antibody, a mouse IgG1, was obtained from Immunotech (Marseilles, France). These monoclonal antibodies were purified from ascites fluids by affinity chromatography on protein A-Sepharose (Pharmacia, Bois d'Arcy, France), as described by the manufacturer. CY34, G7A5, and 679MC7 (2 to 5 mg/ml) were dialyzed once against 10 m*M* formate buffer pH 2.8, 150 m*M* NaCl, then once against 50 m*M* acetate buffer pH 4.2, 150 m*M* NaCl. Pepsin (crystallized twice, Behring Diagnostica, La Jolla, CA), 50 mg per g of antibody, was then added and allowed to react for 2 hr at 37°C. The mixture was fractionated by ion-exchange chromatography on a Mono S column (Pharmacia), equilibrated with 50 m*M* acetate buffer pH 4.5. Elution was performed with a linear gradient of NaCl (0 to 0.6*M*). U7.27 was dialyzed against 10 m*M* acetate buffer pH 3.8 and 50 mg pepsin per g of antibody was added. Digestion was performed over 3 hr at 37°C and stopped by raising the pH to 8 with 1*M* Hepes buffer pH 8.5. The $F(ab')_2$ fragments were first separated from IgG by affinity chromatography on protein A-Sepharose, then loaded onto an AcA 34 gel filtration column (IBF, Paris, France) and eluted in 0.012*M* phosphate buffer, 0.15*M* NaCl, pH 7.2 (PBS). Protein solutions were concentrated by positive pressure ultrafiltration using PM-10 membranes (Amicon, Paris, France). Protein concentrations for IgG, fragments and DSC were determined by optical density at 280 nm (assuming 1.0 mg/ml = 1.4 *A* unit). Purity was assessed by sodium dodecylsulfate-polyacrylamide gel electrophoresis on an automated apparatus (PhastSystem), using 8–25% gradient PhastGels and coomassie blue staining (Pharmacia).

Preparation of DSC

The $F(ab')_2$ fragments of U7.27 or 679MC7 were dialyzed against 0.1*M* phosphate buffer pH 6.0, and cysteamine (Sigma, St. Louis, MO) was added to a final concentration of 10 m*M*. After 1 hr incubation at 37°C, excess cysteamine was removed by gel filtration on a PD10 column (Pharmacia) presaturated with bovine serum albumin (BSA, Fraction V, Bohringer, FRG) and equilibrated in PBS, 5 m*M* ethylenediaminetetraacetic acid (EDTA) pH 7.2 (when oxidized Fab' were desired, a final concentration of 30 m*M* of iodoacetamide (Sigma) was added 30 min before loading on the PD10 column). To the $F(ab')_2$ fragments of CY34 or G7A5 (2 to 5 mg/ml in PBS) was added a tenfold molar excess of N-succinimidyl 3-(2-pyridyldithio)-propionate (SPDP), (Pharmacia, 20 mg/ml in methanol). The mixture was incubated for 1 h at 30°C. Excess SPDP was removed by gel filtration on a PD10 column presaturated with BSA and equilibrated in PBS, 5 m*M* EDTA pH 7.2.

Reduced U7.27 Fab' or 679MC7 Fab' and SPDP-derivatized CY34 or G7A5 $F(ab')_2$ were mixed in a 2 to 1 molar ratio and allowed to react at room temperature for 24 hr. DSCs were separated from unreacted $F(ab')_2$ and Fab' by gel filtration on an AcA 34 column in PBS. Fractions corresponding to an apparent M_r ~150,000 D were collected, pooled, filtered on 0.22 μm filters (Amicon) and stored at 4°C.

Synthesis of N-α-((2,4-dinitrophenyl)-aminocaproyl)-D-tyrosyl-N-ε-((2,4-dinitrophenyl)-aminocaproyl)-D-lysine (di-DNPdTdL), N-α-((2,4-dinitrophenyl)-aminocaproyl)-L-tyrosyl-N-ε-((2,4-dinitrophenyl)-aminocaproyl)-L-lysine (di-DNPTL), di-N-α-N-ε-((2,4-dinitrophenyl)-aminocaproyl)-L-lysyl-L-tyrosine (di-DNPLT), and N-α-((2,4-dinitrophenyl)-amino-caproyl)-tyrosyl-seryl-N-ε-((2,4-dinitrophenyl)-aminocaproyl)-lysine (di-DNPTSL). Three hundred milligrams of DNP-aminocaproic acid (DNP-Cap) (Sigma) were dissolved in 6 ml of dioxane and 120 mg of N-hydroxysuccinimide dissolved in 4 ml of ethyl acetate were added. N,N'-dicyclohexyl-carbodiimide (200 mg in 2 ml of dioxane) was added, and the mixture was allowed to react for 3 hr at room temperature. The precipitate which forms during the reaction was filtered off and the solution was evaporated to dryness under reduced pressure. The yellow residue was crystallized in boiling absolute ethanol. The yellow needles of the N-hydroxysuccinimide ester (DNP-Cap-NHS) were collected and dried (rf = 0.59 by thin layer chromatography on silica gel in chloroform:ethyl acetate, 1:1).

Thirty milligrams of D-tyrosyl-D-lysine, trifluoroacetate (Gift from Dr. G. Gacel, Faculté de Pharmacie, Paris, France), tyrosyl-lysine, lysyl-tyrosine or tyrosyl-seryl-lysine (Bachem, Bubendorf, Switzerland) were dissolved in 0.4 ml of 12.5% sodium carbonate in water pH 9; a twofold molar excess of DNP-Cap-NHS in 2 ml of dioxane was added, and the mixture was allowed to react for 2 hr at room temperature. The mixture was acidified with 1 N HCl and the precipitate was collected. Further purification was obtained by high performance liquid chromatography (HPLC) on a 5 μm ODS ultrosphere reverse phase column (Altex, Berkeley, CA) with a mobile phase of methanol:trifluoroacetic acid (0.05% in water) from 40% to 60% methanol. Purity was assessed by thin layer chromatography in n-butanol:acetic acid:water 4:1:1.

Synthesis of N-α-((2,4-dinitrophenyl)-aminocaproyl)-D-tyrosine (DNPdT) and N-α-((2,4-dinitrophenyl)-amino-caproyl)-L-tyrosine (DNPT). Nine milligrams of D-tyrosine or L-tyrosine (Bachem) were dissolved in 1 ml of 0.2*M* borate buffer pH 8.5 and an equimolar amount of DNP-Cap-NHS in 2 ml of dioxane was added. Further steps were performed as described above.

Synthesis of is-(N-ε-(2,4-dinitrophenyl)-L-lysyl)-diethylenetriaminepentaacetic acid (di-DNPDTPA) and of (N-ε-(2,4-dinitrophenyl)-L-lysyl)-diethylenetriaminepenta-

acetic acid (DNPDTPA). To a solution of DNP-lysine (Sigma, 1.2 mmol in 10 ml of a 1:1 mixture of 100 m*M* borate pH 8.5 and dimethylformamide) were added 0.6 mmol of DTPA cyclic anhydride (Sigma). The mixture was allowed to react overnight at room temperature, then evaporated to dryness under reduced pressure. The residue was dissolved in 10 ml of water and excess HCl (1*M*) was added. The precipitate was redissolved in water by addition of NaOH (1*M*) and further purified by ion exchange chromatography on an FPLC mono Q (Pharmacia) column. di-DNPDTPA had an Rf of 0.15 by thin layer chromatography in n-butanol:acetic acid:water (4:1:1). Some DNPDTPA was formed as a by-product (rf = 0.05). Both products were further purified by HPLC on a reverse phase column using a 1:1 mixture of 0.05% trifluoroacetic acid in water and methanol.

Radiolabeling

DNP concentrations were determined by optical density at 360 nm (assuming 1 m*M* = 17 *A* units). DNP-derivatized peptides (2 nmol) were dissolved in 100 μl of PBS supplemented with 20% ethanol and transferred into a small plastic tube containing 10 μg of Iodogen (Pierce, Rockford, IL), as described by Salacinski and co-workers (*10*). Ten microliter of $Na^{125}I$ (3700 MBq/ml, Du Pont de Nemours, Paris, France) were added and the reaction continued for 30 min at 4°C. The monoiodo-derivatives were purified by HPLC on a reverse phase column with methanol:trifluoroacetic acid (0.05% in water), from 40% to 60% methanol.

To DNPDTPA and di-DNPDTPA (0.25 nmol), dissolved in 0.1 ml of 1*M* citrate buffer pH 5, were added 50 μl of ^{111}In chloride (in 50 m*M* HCl, 148 MBq/ml, NEN). After overnight incubation at room temperature, chelation efficiency was tested, after addition of phosphate, by thin layer chromatography in methanol:10% ammonium acetate in water, 1:1 as described by Meares et al. (*11*). These tracers were stored at 4°C and, just before use, diluted in 10 m*M* Hepes buffer, pH 7.5, 0.1% BSA and 1 m*M* EDTA.

In Vitro Tests

Lymphocytes were obtained from BALB/c or DBA/2 mouse spleens, after red blood cell lysis by ammonium chloride and Ficoll separation. Binding experiments were done as described by Dower and co-workers (*5*): in an Eppendorf plastic tube were incubated 100 μl of a mouse spleen cell suspension (10^8 cells/ml) in Roswell Park Memorial Institute 1640 medium supplemented with 10% fetal calf serum, 25 m*M* Hepes buffer pH 7.2, 0.02% sodium azide and 100 m*M* deoxyglucose, 100 μl of a solution of DSC in PBS 0.1% BSA and 150 μl of radiolabeled hapten solution (10^6 cpm/ml, 0.4 n*M*). After 2 hr at 37°C with agitation, 100 μl of the resulting cell suspension were transferred into triplicate 0.4 ml plastic tubes containing 200 μl of a 1.2:1 mixture of dibutyl-phthalate and ethyl-hexyl-phthalate. After 30 sec centrifugation at 10,000 *g*, 50 μl of the supernatant were collected and counted, and the bottom of the tube, containing the cell pellet, was cut and counted.

In Vivo Tests

Mice were injected i.v. with 0.05 ml of radioactive solutions (0.5 to 2 × 10^7 cpm/ml, 1 to 4 pmol) under mild anaesthesia with ether. When DSC and radiolabeled haptens were co-injected, the mixture was made just before injection. At selected time intervals, injected animals were killed with ether, heart was incised, blood was collected with heparin, and centrifuged for 30 sec at 10,000 *g*. A known volume of plasma was counted. Major organs were dissected and counted in 5 ml tubes. Data on organ relative weights in mice were taken from Covell et al. (*12*).

Calculations

In cell binding experiments, results were expressed as Bound/Free (B/F) ratios. In in vivo studies, data were expressed as the percentage of injected dose (% ID) localized in a given organ (gut was counted with its contents and plasma was evaluated as 0.047 ml per gram of body weight) or, to allow comparison between organs, as the percentage of injected dose per gram of tissue (% ID/g).

RESULTS

Synthesis of DSC and Radiolabeled Haptens

DSC were prepared and purified as described in Materials and Methods. To select those conjugates with one anti-cell antigen $F(ab')_2$ coupled to a single anti-hapten (DNP) Fab', fractions eluting from the AcA 34 gel filtration column at an apparent M_r of 150,000 Da were pooled and used in binding and in vivo experiments. For control experiments, DSC were directly labeled with ^{125}I (*10*). Immunoreactivity towards both Lyb8.2 positive mouse splenocytes and DNP was checked and found essentially equal to that of anti-Lyb8.2 $F(ab')_2$ or anti-DNP Fab' (not shown). Radiolabeled CY34-U7.27 DSC bound BALB/c spleen lymphocytes in vitro with the same affinity constant (7.0 ×

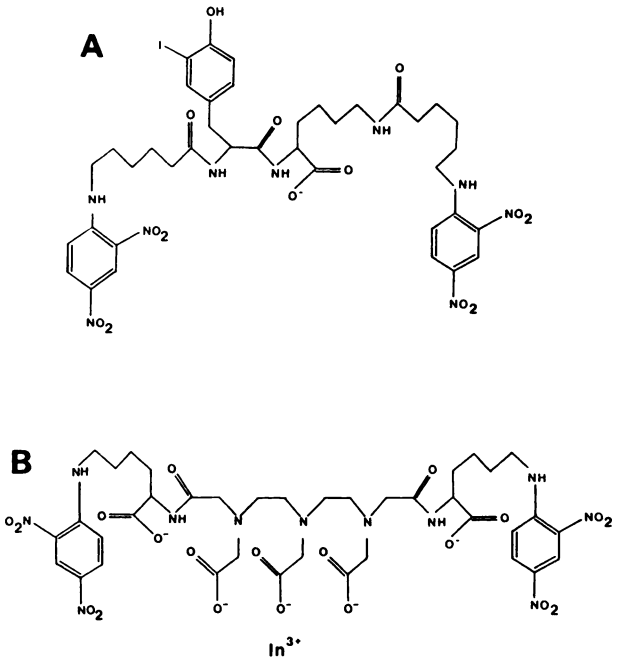

FIGURE 1
Chemical structure of labeled divalent haptens derivatized from N-ε-DNP-aminocaproic acid. A: Iodinated N-α-((2,4-dinitro-phenyl)-aminocaproyl)-D-tyrosyl-N-ε-((2,4-dinitro-phenyl)-amino-caproyl)-D-lysine (di-DNPdTdL). B: Indium labeled bis-(N-ε-(2,4-dinitro-phenyl)-L-lysyl)-diethylene-triamine-pentaacetic acid (di-DNPDTPA).

10^8) as iodinated CY34 IgG (1.8×10^4 sites per B cell). Maximum binding of ^{125}I-DSC was 80% of the maximum binding of CY34 IgG (on BALB/c spleen lymphocytes) and 70% of the maximum binding of U7.27 IgG on DNP-BSA.

DNP-derivatives (Fig. 1) were synthesized as described in Materials and Methods. After labeling with iodine or indium, immunoreactivity measured in the presence of excess anti-DNP monoclonal antibody and poly-ethylene-glycol precipitation was found better than 90%. Iodinated tracers were stable for several weeks at 4°C. Immunoreactivity of indium-labeled tracers was unchanged after 3 days in human serum at 37°C (from 90.6% to 89.8% precipitation for di-DNPDTPA and from 93.5% to 79.8% for DNPDTPA. Nonspecific precipitation, measured without anti-DNP antibody, did not increase).

Divalent and Monovalent Hapten Equilibrium Binding to Monovalent or Divalent Anti-DNP Antibodies

Divalent and monovalent haptens were tested for their ability to inhibit ^{125}I-di-DNPTSL equilibrium binding to CY34-U7.27 DSC. Table 1 shows the 50% displacement concentration for each hapten. Haptens derivatized from D-amino acids have lower affinity than those derivatized from L-isomers, probably because U7.27 monoclonal antibody was obtained after DNP-keyhole lymphet hemocyanin immunization. The divalent haptens used in this study have a somewhat better affinity than the monovalents, explained in part by the statistical factor.

When increasing concentrations of di-DNPTSL (or di-DNPdTdL, or di-DNPTL), were incubated with anti-DNP F(ab')$_2$ and a tracer amount of their ^{125}I-labeled homolog, typical cooperative binding curves were obtained, as shown in Figure 2. This suggests the formation of cyclic complexes <antibody/divalent hapten> (see Discussion). Control experiments, performed with increasing concentrations of monovalent haptens or with anti-DNP F(ab)' did not show such an effect and binding curves could be transformed into linear Scatchard plots (not shown).

Binding of Divalent and Monovalent Haptens on BALB/c Spleen Lymphocytes in the Presence of Increasing Doses of DSC

Iodine-125-labeled divalent and monovalent haptens were tested for binding on BALB/c spleen lymphocytes in the presence of increasing concentrations of CY34-U7.27 DSC (Fig. 3). B/F ratios for the labeled haptens first increased with DSC concentration: DSC (and accordingly DNP binding sites) became bound to the cell surface and permitted the haptens to bind. At DSC concentrations over 1 to 5 n*M* (under the experimental conditions), excess free DSC inhibited hapten binding. Divalent haptens were much more efficient than monovalent at targeting ^{125}I to BALB/c lymphocytes in the presence of DSC (Fig. 3). Similar results were obtained with ^{111}In-labeled tracers (not shown).

Specificity of Hapten Binding to Target Splenocytes in the Presence or Absence of DSC

Nonspecific binding of the haptens to mouse splenocytes was evaluated in the absence of DSC. It was found lower than 3.5% for the divalent and lower than 1.5% for the monovalent haptens. Hapten binding in the presence of DSC was reduced to control levels under the following conditions: addition of excess CY34 IgG, replacement of CY34-U7.27 DSC by G7A5-U7.27 DSC (anti-human melanoma), replacement of BALB/c spleen cells by DBA/2 spleen cells (Lyb8.2 negative), addition of excess di-DNPdTdL or DNPdT, replace-

TABLE 1
Properties of Monovalent and Divalent Haptens

Compound	Inter-DNP distance*	C50 (nM)†	Cyclic Complexes‡	Affinity Enhancement§	% ID in spleen simultaneous¶	% ID in spleen delayed**
DNPdT		15	–	–	0.15 ± 0.02 (5)	ND††
DNPT		5.0	–	–	ND	ND
DNPDTPA		4.5	–	–	1.6 ± 0.3 (5)	3.5 – 3.9 (2)
di-DNPLT	18	4.0	+	+	ND	ND
di-DNPdTdL	32	2.5	+	+	4.5 ± 0.8 (7)	0.39 – 0.41 (2)
di-DNPTL	32	1.0	+	+	6.4 – 7.2 (2)	ND
di-DNPDTPA	34	1.4	+	+	9.6 ± 1.0 (5)	23.0 ± 0.8 (3)
di-DNPTSL	36	0.6	+	+	6.7 – 7.3 (2)	ND

* Fully extended inter-(DNP-amino group) distances were estimated using Ealing CPK values for bond angles and covalent radii.

† Concentration needed for a 50% displacement of ^{125}I-di-DNPTSL equilibrium binding to CY34-U7.27 DSC.

‡ Positive when ^{125}I-di-DNPTSL binding to U7.27 mAb was enhanced by the presence of increasing hapten concentrations (Fig. 2).

§ Positive when B/F for the labeled hapten was higher than B/F for the ^{125}I-DSC in binding assay on BALB/c spleen lymphocytes, in the presence of increasing DSC concentrations (Fig. 3).

¶ Haptens, labeled with ^{125}I or ^{111}In, were injected i.v. to BALB/c mice in the presence of 2 μg of DSC. Mice were killed 1 hr later. Mean from *n* animals, ± s.d. (*n*) when n > 2, otherwise individual results are shown.

** Mice were injected i.v. with the tracers 10 min after a 2-μg DSC injection (i.v.).

†† Not done.

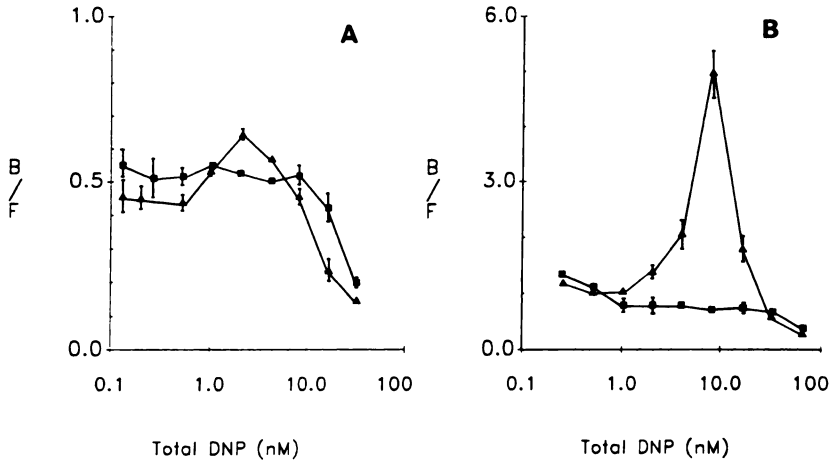

FIGURE 2
Equilibrium binding for increasing amounts of DNPT (A) or di-DNPdTdL (B) to anti-DNP F(ab)'$_2$ (▲, 0.8 μg/ml) or Fab' (■, 3.0 μg/ml). Mixtures of antibody fragments, tracer amounts of ^{125}I-radiolabeled DNPT or di-DNPdTdL (10,000 cpm, 2 10^{-15} mol), and variable concentrations of unlabeled DNP-derivatives were incubated at 37°C for 3 hr and the complexes were precipitated by addition of polyethylene glycol (12.5% final). Each point is the mean of a duplicate ± deviation (unless smaller than the point as plotted).

ment of CY34-U7.27 DSC by CY34-679MC7 (with no anti-DNP reactivity).

Pharmacokinetics and Biodistribution of Directly Labeled DSC in Lyb8.2$^+$ and Lyb8.2$^-$ Animals

After i.v. injection of 200 ng of ^{125}I-labeled CY34-U7.27 DSC in DBA/2 mice (Lyb8.2$^-$), no significant localization was observed in the spleen (0.3 ± 0.1% ID). Distribution of iodine in the major organs and whole-body half-life (~12 hr) were consistent with F(ab)'$_2$-like pharmacokinetics (*13*) (not shown).

When 200 ng of the same ^{125}I-labeled DSC were injected i.v. to BALB/c mice (Lyb8.2$^+$), localization in the spleen occurred within the first hour up to 13 ± 1% of injected dose (185 ± 15% ID)/g). Increasing the injected dose led to a decrease in splenic localization with a half displacement of ~1 μg (Fig. 4). Biodistribution of iodine 1 hr after injection was also consistent with data obtained by Holton et al. (*13*) with ^{125}I-labeled CY34 F(ab)'$_2$ (not shown).

Pharmacokinetics of Labeled Haptens

When ^{125}I-di-DNPTSL, di-DNPTL, di-DNPdTdL or DNPdT were injected i.v. in tracer amounts to BALB/c mice, radioactivity rapidly cleared from plasma (< 6% ID/g at 1 hr) and was trapped by the gut (from 22 to 40% ID/g after 1 hr). This uptake in the gut was not reversed by DNPdT or di-DNPdTdL up to 5 nmol per mouse. Indium-111-di-DNPDTPA or DNPDTPA also rapidly disappeared from plasma (8.0 ± 0.7% ID/g at 1 hr for di-DNPDTPA and 0.5 ± 0.1% ID/g for DNPDTPA) but did not accumulate in any of the organs disected. No localization was observed in the spleen (1.5 and 0.5% ID/g at 1 hr). Whole-body half-lives of divalent haptens were longer than for monovalent but remained below 1.5 hr. Indium-labeled haptens exhibited faster elimination than the iodinated mainly because iodine was trapped by the gut. One-hour plasma antibody-precipitable activities, tested with excess U7.27 IgG, were between 30% and 70%. Immunoreactive products were recovered in the urine, especially with indium-labeled haptens.

DSC Mediated Splenic Uptake of Labeled Haptens in Lyb8.2$^+$ Mice: Kinetics and Specificity

Tracer amounts of ^{125}I- or ^{111}In-labeled haptens were co-injected with 2 μg of CY34-U7.27 DSC in BALB/c mice: rapid splenic localization of radioactivity occurred within the first 30 min followed by a plateau. After 1 hr the percent of dose in spleen decreased rapidly for di-DNPTSL, di-DNPTL or DNPDTPA and more slowly for di-DNPdTdL or di-DNPDTPA with $T_{½}$ of 1 hr and 2 hr, respectively. Maximal uptake was between

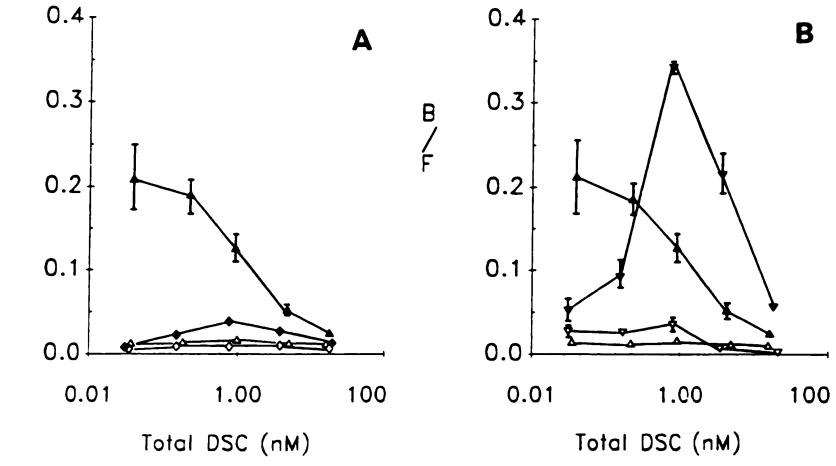

FIGURE 3
Iodine-125-labeled haptens were incubated with BALB/c (closed symbols) or DBA/2 (open symbols) mouse spleen lymphocytes in the presence of increasing concentration of DSC as described in Material and Methods. A: DNPdT (◆, ◇) binding is compared to directly labeled ^{125}I-DSC binding under the same conditions (▲, △). B: di-DNPdTdL (▼, ▽) binding compared to ^{125}I-DSC binding. Each point is the mean of a triplicate ± s.d. (unless smaller than the point as plotted).

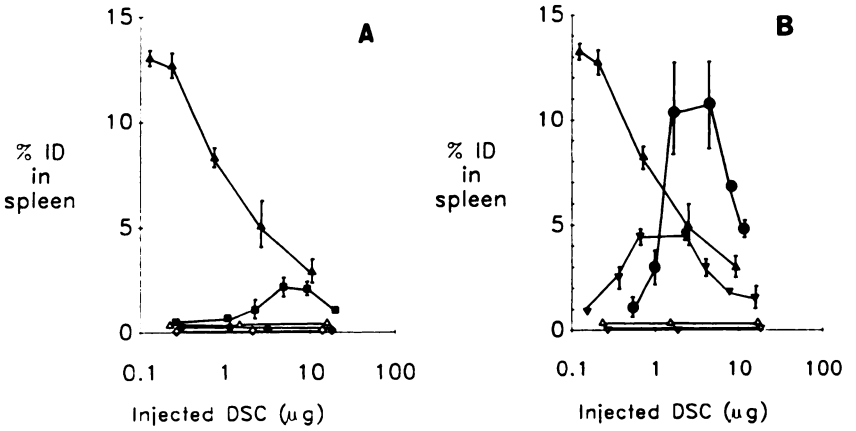

FIGURE 4
A: Localization of ^{125}I-DNPdT (◆, ◇) and of ^{111}In-DNPDTPA (■) in BALB/c (closed symbols) or DBA/2 (open symbols) mouse spleen 1 hr after i.v. co-injection with increasing amounts of DSC. B: Localization of ^{125}I-di-DNPdTdL (▼, ▽) and of ^{111}In-di-DNPDTPA (●). Results are compared with directly labeled ^{125}I-DSC localization under the same conditions (▲, △). Each point is the mean of a duplicate ± deviation (unless smaller than the point as plotted).

4.5 and 9.6% ID (65 to 137% ID/g) for divalent haptens, while it remained below 1.6% ID (23% ID/g) for monovalent haptens (Table 1).

The 1 hr spleen localization of ^{125}I-di-DNPdTdL was below 1.5% ID/g under the following conditions: addition of excess di-DNPdTdL or DNPdT (over 25 pmol of DNP per mouse), replacement of BALB/c mice (Lyb8.2$^+$) by DBA/2 (Lyb8.2$^-$) mice.

Localization of ^{125}I- or ^{111}In-Labeled Divalent and Monovalent Haptens in Spleen 1 hr After Co-injection with Increasing Doses of DSC

BALB/c mice were co-injected with increasing doses of CY34-U7.27 DSC and a constant tracer amount of ^{125}I-di-DNPdTdL (or DNPdT) or ^{111}In-di-DNPDTPA (or DNPDTPA). Radioactivity uptake in spleen is shown in Figure 4 as a function of DSC injected dose: bell shaped curves for hapten uptakes were similar to that obtained in cell binding experiments (Fig. 3). Indeed, the spleen uptake of the labeled haptens first increased with DSC injected dose: DSC bound to spleen cells and mediated hapten binding. When DSC injected dose was further increased over 2 to 5 μg, hapten uptake decreased as excess free DSC inhibited hapten binding.

Figure 4 also shows that divalent haptens are much more efficient than monovalent at localizing in the spleen in the presence of CY34-U7.27 DSC, especially when a same class of labeled haptens is considered (e.g., di-DNPDTPA and DNP-DTPA).

Radioactivity biodistribution 1 hr (respectively, 2 hr) after co-injection of ^{125}I-di-DNPdTdL (respectively ^{111}In-di-DNPDTPA) and 2 μg of CY34-U7.27 DSC to BALB/c mice is shown in Figure 5 and compared to controls.

Two-Step Administration of DSC and Radiolabeled Haptens

BALB/c mice were injected i.v. with 2 μg of CY34-U7.27 DSC and, after a variable delay, with tracer amount of ^{125}I-di-DNPdTdL, ^{111}In-di-DNPDTPA, or DNPDTPA. Radioactive uptake in spleen and major organs 30 min or 1 hr after the tracer injection are shown in Figure 6. Iodine uptake in spleen was reduced when ^{125}I-di-DNPdTdL and DSC were not mixed just before injection. By contrast, indium uptakes were increased when di-DNPDTPA (or DNPDTPA) and the DSC were injected sequentially. Whatever the tracer, uptake in spleen decreased with the delay between DSC and tracer injection with a $T_{1/2}$ of 15 to 30 min, suggesting that the cell-bound anti-DNP activity disappeared with time.

DISCUSSION

In order to design "affinity enhancement" tracers (i.e., with more affinity to cell-bound than to unbound DSC) able to target radioisotopes to the cell surface in the presence of excess free DSC, we synthesized DNP-derived divalent haptens capable of cross-linking a soluble (divalent) anti-DNP mAb. The fact that divalent haptens can cross-link divalent antibodies has already been reported (*14*). When cyclic complexes are formed, plots such as that shown in Figure 2 may be predicted by computer simulation (*15*). Such cooperative effects cannot be explained by the formation of linear polymers only (*16*). This strongly suggests that all the dimers we tested may be involved in cyclic complexes where two anti-DNP mAbs are bound to a single divalent hapten molecule (Table 1).

The possibility of antibody cross-linking was a prerequisite to the affinity enhancement approach: if divalent haptens can cross-link soluble anti-DNP mAb, they should be able to cross-link two cell bound DSC by formation of ⟨membrane/Lyb8.2/DSC/hapten/DSC/Lyb8.2/membrane⟩ complexes (Fig. 7). The formation of such complexes should increase divalent hapten apparent affinity to cell-bound DSC when compared to free DSC (monovalent with respect to DNP binding). As a consequence, divalent haptens bind the cells with "affinity enhancement", i.e., display selectivity for cell-bound, as opposed to excess free, DSC: this is best demonstrated by the observation that divalent hapten B/F ratios, for intermediate and high DSC con-

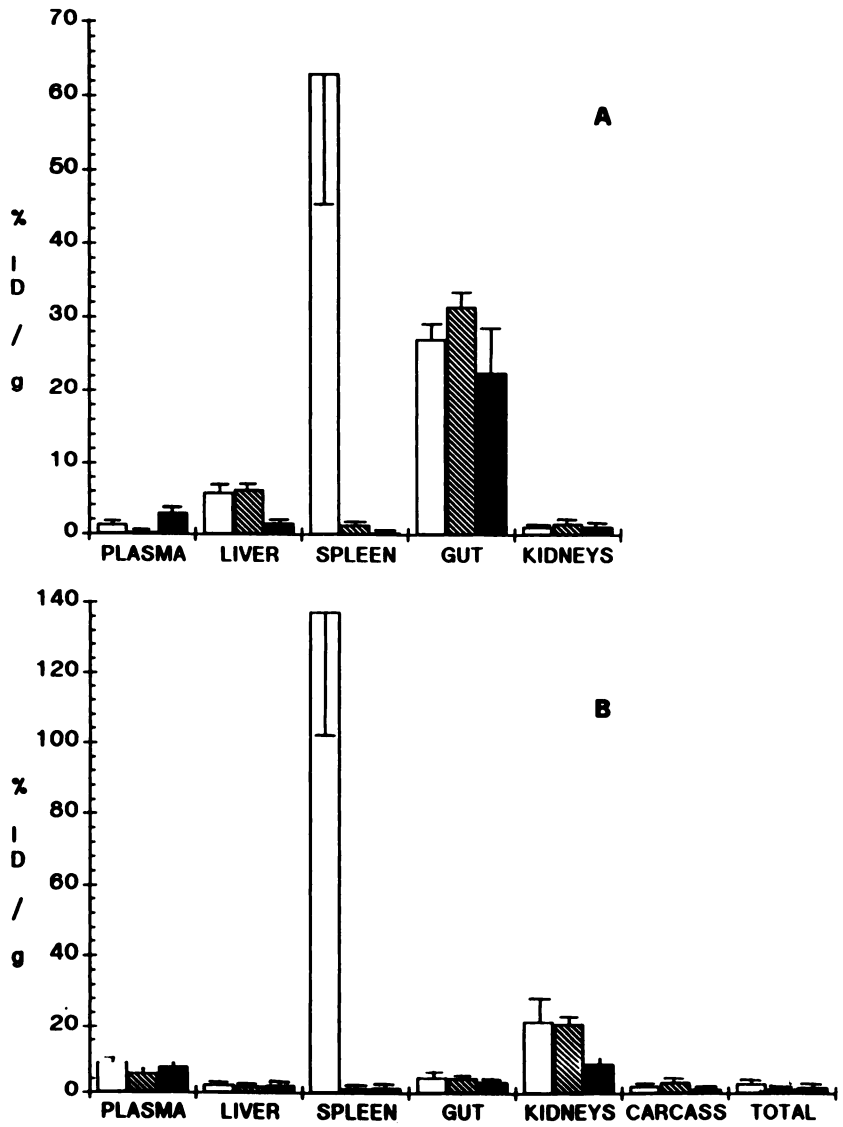

FIGURE 5
Biodistribution of labeled divalent haptens in BALB/c (□) or DBA/2 (▨) mice after i.v. co-injection with 2 μg of DSC. A: ^{125}I-di-DNPdTdL 1 hr after injection (n = 7 and 3 respectively, ± s.d.). B: ^{111}In-di-DNPDTPA 2 hr after injection (n = 3 and 2, respectively, ± s.d.). (■): control tracer distributions in BALB/c, without DSC (n = 3, ± s.d.).

centrations, were higher than the B/F ratio obtained with directly labeled CY34-U7.27 DSC under the same experimental conditions (Fig. 3). Affinity enhancement was only observed with divalent haptens: B/F obtained with monovalent haptens are always smaller (even when divalent and monovalent hapten affinity to soluble DSC are in the same range, Table 1).

Under the experimental conditions, affinity enhancement is advantageous in a DSC concentration range of 5 nM to 50 nM (0.75 to 7.5 μg/ml). These concentrations are achieved in vivo after i.v. administration of 1.5 to 15 μg of DSC in mice. As in vivo DNP binding to anti-DNP monoclonal antibody has already been reported (*17*), the only condition to use the affinity enhancement effect in vivo was to prepare reasonably stable labeled divalent haptens. Indium-111 DTPA derivatives are convenient with this respect: they do not accumulate in nontarget organs and remain immunoreactive after injection. When co-injected with various amounts of DSC, the divalent tracer performs much better than the monovalent, with maximal specific uptake up to 11% ID (compared to 2%). Indium-111-di-DNPDTPA, co-injected with high amounts of DSC, localizes in spleen better than ^{125}I-DSC under the same conditions (see Fig. 4): this suggests that affinity enhancement may occur in vivo as well.

Lower localization is obtained with ^{125}I-labeled haptens. This can be explained by the rapid gut trapping observed for these haptens. In this case, it is not clear whether the better localization of di-DNPdTdL, when compared to DNPdT, is related to affinity enhancement, to better affinity for the DSC (Table 1), or to more suitable pharmacokinetic properties (DNPdT is less hydrophobic than di-DNPdTdL as it contains only one DNP group).

To take maximum advantage of indirect targeting, labeled hapten injection should follow DSC injection: hapten trapping by excess free DSC should be lower if no <hapten/DSC> complexes are formed before injection. Indeed, ^{111}In uptake in the spleen increases up to

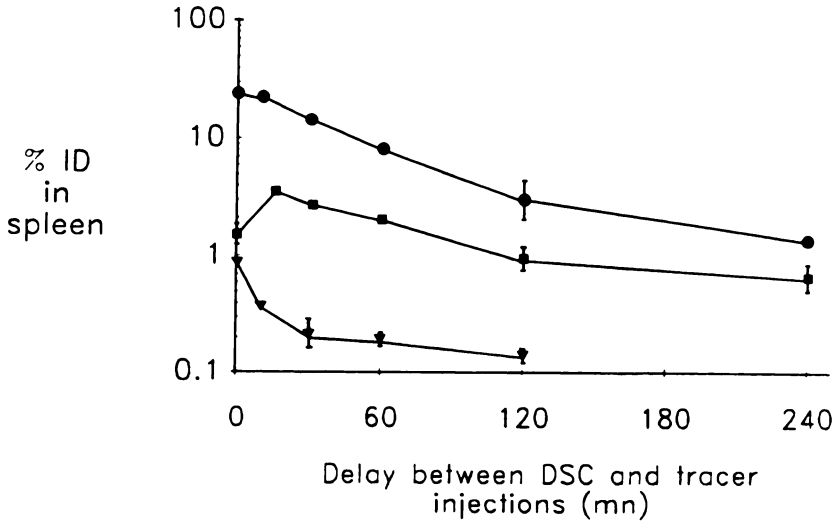

FIGURE 6
Localization of ^{125}I-di-DNPdTdL (▼), ^{111}In-di-DNPDTPA (●) and ^{111}In-DNPDTPA (■) in BALB/c mouse spleen. Two micrograms of DSC were first injected i.v. Then, after a variable delay (abscissa), mice were injected with the tracers and killed 1 hr later (30 min for DNPDTPA). Each point is the mean of a duplicate ± deviation (unless smaller than the point as plotted).

23% ID (328% ID/g) when di-DNPDTPA is injected 10 min after an optimal dose of DSC (Fig. 6). By contrast, spleen localization of ^{125}I-di-DNPdTdL is reduced to 0.4% ID (5.7% ID/g) when this injection protocol is applied: reasonable localization can only be achieved when pre-formed ⟨^{125}I-di-DNPdTdL/DSC⟩ complexes are injected, perhaps because the tracer is then partly protected from gut trapping. This is consistent with some data obtained in vitro suggesting that preformed ⟨hapten/DSC⟩ complexes dissociate within ~5 min under conditions close to that of in vivo administration (i.e., 37°C and pure mouse serum, data not shown). However, Figure 6 shows that DSC availability for hapten binding rapidly disappears from spleen cells, so that this model system is not adequate to test the effect of long delays (between DSC and tracer injections) on tracer localization.

In addition, after spleen uptake in Lyb8.2$^+$ animals, iodine is released rather rapidly from the spleen. This effect was also reported with ^{125}I-labeled CY34 IgG, F(ab')$_2$, and Fab' within the same time scale (*13*). Indium targeted to the spleen by means of DSC is also released. This is in contrast to the general observation that ^{111}In targeted by chelate-labeled monoclonal antibody or fragments remains localized for extended periods of time (*18*). This suggests that In-labeled haptens are handled by the target cells in a different way than chelate-labeled antibodies.

In any case, ^{125}I- or ^{111}In-labeled divalent or monovalent haptens bind to spleen lymphocytes in the presence of DSC only if DSC has both anti-Lyb8.2 and anti-DNP reactivity, and only if cells express the Lyb8.2 antigen. This was clearly observed both in vitro and in vivo. In vivo, however, inadequate pharmacokinetic properties of iodinated haptens dramatically reduced their targeting ability. This could be prevented by altering the chemical structure, for example by using a different substrate for iodination. Increasing the hydrophilicity of the molecule may also increase the specificity of the tracers. Experiments in this direction are in progress: since the absolute requirements on the tracers for affinity enhancement are the presence of two (or more) hapten groups and of a site for radiolabeling, the possibilities for the design of better tracers are plentiful. As an example, the ^{111}In-labeled tracers work much better, probably because of higher hydrophilicity and in vivo stability. Actually, the only significant site of nonspecific localization was the kidneys, which was not unexpected since kidneys are the preferential elimination route for F(ab')$_2$, Fab' (the components of the DSC) and of ^{111}In-DTPA, as well as the classical sites of nonspecific uptake for ^{111}In directly labeled monoclonal antibody fragments.

The results obtained with ^{111}In-labeled divalent hapten are comparable to specific localization obtained with directly labeled antibodies or fragments in similar model systems using differentiation antigens as targets.

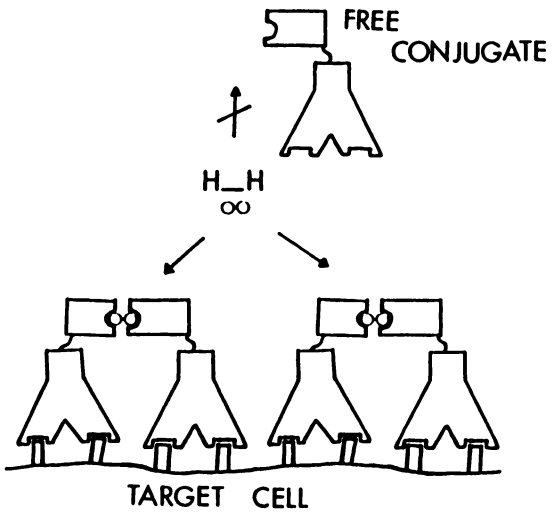

FIGURE 7
Schematic representation of probable complexes formed on the cell surface by DSC and bivalent haptens (H-H).

For instance, Houston et al. (*19*) obtained 20% ID/g in the spleen and 50% ID/g in lymph nodes with an anti-Thy1.1 $F(ab')_2$ and Goodwin et al. (*20*) 120% ID/g in the spleen with an anti-I-A^k. With CY34 itself, Holton et al. (*13*) obtained up to 40% ID (571% ID/g) localized in the spleen. Further comparisons between direct and two-step targeting techniques (especially in terms of contrast), should be carried on with other animal models (as tumor bearing mice). Indeed, contrast improvement is really needed when the fraction of injected antibody delivered to the target is <10% per g. However, the results presented here suggest that the use of divalent haptens (allowing affinity enhancement) may improve two-step targeting techniques and, consequently, in vivo radioimmunoimaging and radioimmunotherapy.

ACKNOWLEDGMENTS

The authors thank Raymond Cesaroni for animal care, and all the staff at Immunotech for enthusiastic support.

REFERENCES

1. Reardan DT, Meares CF, Goodwin DA, et al. Antibodies against metal chelates. *Nature* 1985; 316:265–268.
2. Goodwin DA, Meares CF, David GS, et al. Monoclonal antibodies as reversible equilibrium carriers of radiopharmaceuticals. *Int J Nucl Med Biol* 1986; 13: 383–391.
3. Goodwin DA, Meares CF, McTigue M, David GS. Monoclonal antibody hapten radiopharmaceutical delivery. *Nucl Med Comm* 1986; 7:569–580.
4. Goodwin DA, Meares CF, McCall MJ, McTigue M, Chaovapong W. Pre-Targeted immunoscintigraphy of murine tumors with indium-111-labeled bifunctional haptens. *J Nucl Med* 1988; 29:226–234.
5. Dower SK, DeLisi C, Titus JA, Segal DM. Mechanism of binding of multivalent immune complexes to Fc receptors. I. Equilibrium binding. *Biochemistry* 1981; 20:6326–6334.
6. Segal DM, Guyer RL, Plotz PH. Complement fixation by model immune complexes free in solution and bound onto cell surfaces. *Biochemistry* 1979; 18: 1830–1835.
7. Capelle N, Barbet J, Dessen P, Blanquet S, Roques BP, Le Pecq JB. Deoxyribonucleic acid bifunctional intercalators: kinetic investigation of the binding of several acridine dimers to deoxyribonucleic acid. *Biochemistry* 1979; 18:3354–3362.
8. Portoghese PS, Larson DL, Sayre LM, et al. Opioid agonist and antagonist bivalent ligands. The relationship between spacer length and selectivity at multiple opioid receptors. *J Med Chem* 1986; 29:1855–1861.
9. Symington FW, Subbarao B, Mosier DE, Sprent J. Lyb-8.2: a new B cell antigen defined and characterized with a monoclonal antibody. *Immunogenetics* 1982; 16:381–391.
10. Salacinsky PRP, McLean P, Sykes JEC, Clement-Jones VV, Lowry PJ. Iodination of proteins, glycoproteins and peptides using a solid phase oxidizing agent 1,3,4,6-tetra-chloro-3,6-diphenyl glycoluryl (Iodogen). *Anal Biochem* 1981; 117:136–141.
11. Meares CF, McCall MJ, Reardan DT, Goodwin DA, Diamanti CI, McTigue M. Conjugation of antibodies with bifunctional chelating agents: isothiocyanate and bromoacetamide reagents, methods of analysis, and subsequent addition of metal ions. *Anal Biochem* 1984; 142:68–78.
12. Covell DG, Barbet J, Holton OD, Black CDV, Parker RJ, Weinstein JN. Pharmacokinetics of monoclonal immunoglobulin G_1, $F(ab)'_2$, and Fab' in mice. *Cancer Res* 1986; 46:3969–3978.
13. Holton OD III, Black CDV, Parker RJ, et al. Biodistribution of monoclonal IgG_1, $F(ab')_2$, and Fab' in mice after intravenous injection. Comparison between anti-B cell (anti-Lyb8.2) and irrelevant (MOPC-21) antibodies. *J Immunol* 1987; 139:3041–3049.
14. Valentine RC, Green NM. Electron microscopy of an antibody-hapten complex. *J Mol Biol* 1967; 27:615–623.
15. Wofsy C, Goldstein B. The effect of co-operativity on the equilibrium binding of symetric bivalent ligands to antibodies: theoretical results with application to histamine release from basophils. *Mol Immunol* 1987; 24:151–161.
16. Steward MW, Steensgaard J. In: Antibody affinity: thermodynamical aspects and biological significance, Chap. 1. Boca Raton, Florida: CRC Press Inc, 1983.
17. Aragnol D, Leserman LD. Immune clearance of liposomes inhibited by an anti-Fc receptor antibody in vivo. *Proc Natl Acad Sci USA* 1986; 83:2699–2703.
18. Khaw BA, Cooney J, Edgington T, Strauss HW. Differences in experimental tumor localization of dual-labeled monoclonal antibody. *J Nucl Med* 1986; 27: 1293–1299.
19. Houston LL, Nowinski RC, Bernstein ID. Specific in vivo localization of monoclonal antibodies directed against the Thy1.1 antigen. *J Immunol* 1980; 125: 837–843.
20. Goodwin DA, Meares CF, McCall MJ, et al. Chelate conjugates of monoclonal antibodies for imaging lymphoid structures in the mouse. *J Nucl Med* 1985; 26:493–502.